J. Fluid Mech. (1996), *vol.* 313, *pp.* 131–145

Theory of low Mach number compressible flow in a channel

By A. SHAJII AND J. P. FREIDBERG

Plasma Fusion Center, Massachusetts Institute of Technology, Cambridge, MA 02139, USA

(Received 22 February 1995 and in revised form 3 November 1995)

The properties of a relatively uncommon regime of fluid dynamics, low Mach number compressible flow are investigated. This regime, which is characterized by an exceptionally large channel aspect ratio $L/d \sim 10^6$ leads to highly subsonic flows in which friction dominates inertia. Even so, because of the large aspect ratio, finite pressure, temperature, and density gradients are required, implying that compressibility effects are also important. Analytical results are presented which show, somewhat unexpectedly, that for forced channel flow, steady-state solutions exist only below a critical value of heat input. Above this value the flow reverses against the direction of the applied pressure gradient causing fluid to leave both the inlet and outlet implying that the related concepts of a steady-state friction factor and heat transfer coefficient have no validity.

1. Introduction

This paper describes the basic properties of a relatively uncommon regime of fluid dynamics, low Mach number compressible flow (LMCF). Such flows have distinctly different behaviour than the more familiar and extensively investigated regimes of high Mach number compressible flow (of great interest to aerodynamicist) and low Mach number incompressible flow (of great interest to many mechanical engineering applications).

The motivation to study the LMCF regime results from research (Shajii & Freidberg 1994*a*, *b*) on the cooling of large-scale superconducting magnets such as might be used in next generation magnetic fusion experiments (Thome 1994). A typical magnet coil has a large diameter on the order of 15 m. Because of the need for electrical continuity of the superconductor each N-turn coil is fabricated from a single, uninterrupted length of cable $L \approx 1$ km. The cross-section of the cable is circular with a radius $R_c \approx 2$ cm. The cable itself is composed of approximately 1000 tightly compacted, twisted superconducting/copper strands, each strand having a radius $R_s \approx 0.5$ mm. The coil is cooled by supercritical helium flowing between the strands. With regard to the fluid dynamic behaviour of the coolant, the geometry implies that the hydraulic diameter d for the flow is comparable to the strand diameter: $d \approx 1$ mm. That is, the combination of a large wetted perimeter and a typical void fraction of ≈ 0.4 causes d to be much less than R_c but comparable to R_s. Consequently, the aspect ratio of the flow has the enormous value $L/d \approx 10^6$.

This is the crucial property of LMCF. With such a large aspect ratio, the flow is dominated by friction rather than inertia. The resulting flows are highly subsonic: $M \sim 0.02$. Even so, because of the long lengths involved, a finite pressure gradient is required to drive the flow. Thus, the usual equivalence of low Mach number and incompressible flow (White 1986) does not apply: even though $M \ll 1$, the finite

gradients in p, ρ, and T imply that compressibility is an important effect that must be included in the modelling.

Of the many areas of fluid dynamics that have been studied, two that are related to LMCF are that of gaseous flow through a porous medium (Kaviany 1991), and creeping flow through consolidated media. Gaseous porous-medium flow is more closely related in that the flows are subsonic and compressibility must be included. However, in the analytical investigations thus far presented (mainly corresponding to flow in capillary tubes) the ratio L/d while large, is not so large that finite pressure gradients are required (Kaviany 1991; Zanotti & Carbonell 1984). The compressibility could thus be treated perturbatively about an incompressible state, with $\Delta p/p$ being the expansion parameter (Prud'homme, Chapman & Bowen 1986; Prins 1991). Even with small compressibility it was shown that important modifications arise in the laminar pressure and velocity profiles (Prud'homme *et al.* 1986; Prins 1991; Berg, Seldam & Gulik 1993). More recently, numerical studies have been initiated to analyse non-isothermal compressible flow and heat transfer in cylindrical packed beds (Foumeny & Ma 1994). Considerable research has been carried out on creeping flow, but most of the work has concentrated on incompressible flow (White 1991).

The work described here assumes $M \ll 1$ and $\Delta p/p \sim \Delta T/T \sim \Delta\rho/\rho \sim 1$. As an initial attempt to understand the flow properties of the LMCF regime we focus on the problem of steady-state laminar flow of an ideal gas in a channel. However, since most superconducting magnet applications are characterized by turbulent flow, we include such effects, but only in the simplified context of a turbulent friction factor. The goals are to (i) determine the basic flow and heat removal properties of the gas, (ii) develop an understanding of the corresponding friction factor and heat transfer coefficient and how they might be measured experimentally in the laminar regime, and (iii) develop insight into some of the effects of turbulence on the flow. A number of new and somewhat surprising results follow from the analysis and are summarized below.

(i) A basic LMCF ordering is defined from which we derive the nonlinear, time-dependent LMCF model.

(ii) Analytic solutions are obtained for the flow properties in the case $\mu = \text{const.}$ and $\kappa = \text{const.}$ (here μ is the viscosity and κ is the thermal conductivity).

(iii) The analytic solutions are generalized to the more realistic case $\mu = \mu(T)$ and $\kappa = \kappa(T)$. In this situation there exist two bifurcated solutions, only one of which is stable.

(iv) It is demonstrated that experimental measurements of the friction factor f and heat transfer coefficient h are coupled. For instance to determine f, not only are the flow rate and pressure drop required, but one must also measure the inlet and outlet temperatures and the applied heat flux. A similar consideration applies to h.

(v) Somewhat surprisingly, for a given pressure drop Δp, steady-state solutions (and the corresponding concepts of a steady-state friction factor and heat transfer coefficient) exist only when the applied heat flux lies below a critical value: $q < q_c$. For $q > q_c$, the flow never reaches steady state. Instead, at some point in the channel, the flow reverses against the applied pressure gradient. Fluid then flows out of both the inlet and outlet quickly depleting the system of coolant.

(vi) For the more realistic case $\mu = \mu(T)$, $\kappa = \kappa(T)$, it is shown that in conjunction with the condition $q < q_c$, there is an additional requirement that the mass flow satisfy $\dot{m} > \dot{m}_c$. Attempts to measure f and h at low flow rates again lead to flow reversal and depletion of the gas.

(vii) The effects of turbulence are modelled by introducing a friction factor in place of the laminar viscosity. The qualitative nature of the flow remains unchanged

although the value of q_c is reduced relative to its laminar value as the Reynolds number is increased. The phenomena described above are thus not pathologies of laminar flow.

The analysis leading to these conclusions is described in the main body of the text.

2. Model

The starting point for the analysis is the set of general mass, momentum, and energy conservation laws for an ideal, compressible, monatomic gas. The corresponding equations are given by (Bird, Stewart & Lightfoot 1960)

$$\frac{\partial \rho}{\partial t} + \nabla \cdot \rho \boldsymbol{v} = 0, \tag{1}$$

$$\rho\left(\frac{\partial \boldsymbol{v}}{\partial t} + \boldsymbol{v} \cdot \nabla \boldsymbol{v}\right) = -\nabla p - \nabla \cdot \boldsymbol{\tau}, \tag{2}$$

$$\rho C_v\left(\frac{\partial T}{\partial t} + \boldsymbol{v} \cdot \nabla T\right) + \rho C_\beta T \nabla \cdot \boldsymbol{v} = -\nabla \cdot \boldsymbol{q} - \boldsymbol{\tau} : \nabla \boldsymbol{v}, \tag{3}$$

$$p = R\rho T. \tag{4}$$

For the gas under consideration $C_v = \frac{3}{2}R$ and $C_\beta = R$. The stress tensor and heat flux have their usual forms:

$$\boldsymbol{\tau} = -\mu[\nabla \boldsymbol{v} + (\nabla \boldsymbol{v})^T] + \tfrac{2}{3}\mu(\nabla \cdot \boldsymbol{v})\boldsymbol{I},$$

$$\boldsymbol{q} = -\kappa \nabla T,$$

where $\boldsymbol{I}$ is the identity tensor and μ and κ are assumed to be functions of T.

Consider the regime of low Mach number compressible flow (LMCF), a situation that arises when the length of a channel L is sufficiently large with respect to its hydraulic diameter d. In this regime the frictional force due to viscosity dominates inertial effects, leading to a low Mach number flow even though the pressure gradient is finite. The practical conditions under which this occurs correspond to

$$v \sim \frac{pd^2}{\mu L} \ll v_s \tag{5a}$$

or equivalently

$$M^2 \sim \frac{d}{L} Re \ll 1 \tag{5b}$$

where $M = v/v_s$ is the Mach number and $Re = \rho v d/\mu$ is the Reynolds number. Note that we are concerned with flow gradients occurring over the entire length of the channel L. A different scaling would be required for short-scale entrance problems.

When (5) is satisfied the basic model can be easily recast in a dimensionless form containing only three dimensionless parameters: M^2, (d/L), and the Prandtl number $Pr = C_p \mu/\kappa$ which is always on the order of unity for gases. Based on the above discussion one can now introduce a basic ordering scheme that defines low Mach number compressible flow:

$$\frac{v_\perp}{v_z} \sim \frac{d}{L} \sim \frac{1}{\nabla_\perp}\frac{\partial}{\partial_z} \sim M^4 \sim \epsilon \ll 1, \tag{6a}$$

$$\frac{L}{v_z}\frac{\partial}{\partial t} \sim \frac{\mu L v_z}{pd^2} \sim \frac{\Delta p}{p} \sim \frac{\Delta T}{T} \sim \frac{\Delta \rho}{\rho} \sim Pr \sim 1. \tag{6b}$$

Here Δp, ΔT, $\Delta \rho$ are the changes in p, T, ρ from inlet to outlet, and the subscripts z and $\perp$ refer to the parallel and transverse flow directions respectively. For convenience ϵ has been introduced as a formal ordering parameter.

As a reference case, consider a small-scale hypothetical test experiment using helium as the gas. The relevant parameters are $d = 10^{-3}$ m, $L = 10^2$ m, ρ (inlet) = 1.4 kg m^{-3}, T (inlet) = 100 K, $\Delta p = 2 \times 10^5$ N m^{-2}, $\Delta p/p$ (inlet) = $\frac{2}{3}$, v_s (inlet) = 590 m s^{-1}, and μ (inlet) = 9.6×10^{-6} kg m^{-1} s^{-1}. It can easily be shown that these parameters satisfy the requirements of the LMCF ordering.

The next step is to substitute the ordering scheme into the basic model. To obtain a closed set of equations we require the following variables to the order indicated:

$$\rho = \rho_0 + \ldots, \quad \boldsymbol{v} = (\boldsymbol{v}_{\perp 2} + \ldots) + (v_{z1} + \ldots)\boldsymbol{e}_z, \tag{7a, b}$$

$$p = p_0 + p_2 + \ldots, \quad T = T_0 + T_1 + \ldots, \tag{7c, d}$$

where for any quantity $Q, Q_n \sim \epsilon^n Q_0$. Observe that we require only the first non-vanishing terms for $\rho, \boldsymbol{v}_\perp$ and v_z but require higher-order corrections for p and T. (The first-order correction p_1 vanishes trivially.) The reasons for this will become apparent as the analysis progresses.

Consider first the mass equation. In the context of the LMCF expansion this equation remains unchanged as all terms are competitive. Continuing, in the perpendicular component of the momentum equation, the leading-order contribution is given by

$$\nabla_\perp p_0 = 0 \tag{8a}$$

or equivalently

$$p_0 = p_0(z, t). \tag{8b}$$

To leading order the pressure is constant in the cross-section. The first higher-order non-vanishing contribution can be written as

$$\nabla_\perp \tilde{p_2} = \mu[\nabla_\perp^2 \boldsymbol{v}_{\perp 2} + \tfrac{1}{3}\nabla_\perp(\nabla \cdot \boldsymbol{v})] - \frac{\partial \mu}{\partial z}\nabla_\perp v_{z1} - \nabla_\perp \mu \cdot [\tfrac{2}{3}(\nabla \cdot \boldsymbol{v})\boldsymbol{I} - \nabla_\perp \boldsymbol{v}_{\perp 2} - (\nabla_\perp \boldsymbol{v}_{\perp 2})^T]. \tag{9}$$

This complicated equation is required to determine the transverse dependence of the pressure.

For the parallel component of the momentum equation, only the leading-order contribution is necessary:

$$\frac{\partial p_0}{\partial z} = \nabla_\perp \cdot (\mu \nabla_\perp v_{z1}). \tag{10}$$

From (9) and (10) we see that in the context of the LMCF ordering, inertia is negligible relative to viscous forces.

The next relation of interest is the energy equation. To leading order this reduces to

$$\nabla_\perp \cdot (\kappa \nabla_\perp T_0) = 0. \tag{11}$$

For channel problems the solution to (11) is $T_0 = T_0(z)$ and one must calculate to higher order to determine the transverse heat flux. In annular or slab problems with large transverse heat flow the entire solution can be obtained in leading order. In the application sections we consider the more interesting case $T_0 = T_0(z)$. For this class of problems, where the temperature is nearly constant in the cross-section, we require the first higher-order non-vanishing contribution, which can be written as

$$\tfrac{3}{2}\rho_0 R\left(\frac{\partial T_0}{\partial t} + \boldsymbol{v} \cdot \nabla T_0\right) + p_0 \nabla \cdot \boldsymbol{v} = \nabla_\perp \cdot (\kappa \nabla_\perp T_1) + \mu(\nabla_\perp v_{z1})^2. \tag{12}$$

Observe that both compression and frictional heating are included in the energy equation.

The final relation of interest is the equation of state which requires only the leading-order contribution. For convenience, we summarize the LMCF equations below:

$$\frac{\partial \rho}{\partial t} + \nabla \cdot \rho \boldsymbol{v} = 0, \tag{13}$$

$$\nabla_\perp p_2 = \mu[\nabla_\perp^2 \boldsymbol{v}_\perp + \tfrac{1}{3}\nabla_\perp(\nabla \cdot \boldsymbol{v})] - \frac{\partial \mu}{\partial z}\nabla_\perp v_z - \nabla_\perp \mu \cdot [\tfrac{2}{3}(\nabla \cdot \boldsymbol{v})\boldsymbol{I} - \nabla_\perp \boldsymbol{v}_\perp - (\nabla_\perp \boldsymbol{v}_\perp)^T], \tag{14}$$

$$\frac{\partial p}{\partial z} = \nabla_\perp \cdot (\mu \nabla_\perp v_z), \tag{15}$$

$$\nabla_\perp \cdot (\kappa \nabla_\perp T) = 0, \tag{16}$$

$$\tfrac{3}{2}\rho R\left(\frac{\partial T}{\partial t} + \boldsymbol{v} \cdot \nabla T\right) + p \nabla \cdot \boldsymbol{v} = \nabla_\perp \cdot (\kappa \nabla_\perp T_1) + \mu(\nabla_\perp v_z)^2, \tag{17}$$

$$p = R\rho T, \tag{18}$$

where for simplicity all subscripts have been suppressed except on p_2 and T_1. The basic unknowns in the problem are $\rho, p, T, \boldsymbol{v}, p_2$ and T_1. All quantities are functions of (x, y, z, t) except $p = p(z, t)$. Although there appear to be seven equations and eight unknowns, the fact that p depends only on (z, t) allows the problem to be ultimately evaluated by means of an integrability condition on (17).

The specific applications discussed in the paper are concerned with steady-state two-dimensional fully developed laminar flow in a straight circular channel. Under these conditions, the LMCF model reduces to

$$\nabla \cdot \rho \boldsymbol{v} = 0, \tag{19}$$

$$\frac{\partial p}{\partial z} = \frac{1}{r}\frac{\partial}{\partial r}\left(r\mu \frac{\partial v_z}{\partial r}\right), \tag{20}$$

$$\frac{1}{r}\frac{\partial}{\partial r}\left(r\kappa \frac{\partial T}{\partial r}\right) = 0, \tag{21}$$

$$\tfrac{3}{2}\rho R \boldsymbol{v} \cdot \nabla T + p \nabla \cdot \boldsymbol{v} = \frac{1}{r}\frac{\partial}{\partial r}\left(r\kappa \frac{\partial T_1}{\partial r}\right) + \mu\left(\frac{\partial v_z}{\partial r}\right)^2, \tag{22}$$

$$p = R\rho T. \tag{23}$$

Here, $\boldsymbol{v} = v_r \boldsymbol{e}_r + v_z \boldsymbol{e}_z$, and ρ, T, T_1 and $\boldsymbol{v}$ are functions of (r, z). The pressure $p = p(z)$ is determined by means of an integrability condition on (22). The equation for p_2 is not explicitly needed for the problems under consideration. Equations (19)–(23) describe low Mach number compressible flow and serve as the basis for the analysis that follows.

3. Flow in a channel

In this section the LMCF properties in a straight circular channel are investigated. The specific problem of interest assumes that a uniform (in z) heat flux q is applied along the entire length of the channel. As previously stated, the channel is sufficiently long that entrance efforts can be neglected. The goals of the analysis are to calculate

the flow rate as a function of applied pressure gradient and the outlet temperature as a function of q and the inlet temperature. In contrast to incompressible flow it is shown that the evaluation of the flow rate $\dot{m}$ and exit temperature T_e are coupled, with $\dot{m}$ a function of q and T_e a function of Δp. Once the solutions are obtained, a short calculation is presented giving the LMCF friction factor and Nusselt number, which are then compared to the corresponding incompressible results.

3.1. *Analysis*

The analysis proceeds as follows. Since p is only a function of z, (20) can be immediately integrated with respect to r, leading to a Poiseuille-like profile for the parallel velocity

$$v_z(r,z) = -\frac{p'b^2}{4\mu}\left(1-\frac{r^2}{b^2}\right). \tag{24}$$

Here, the prime denotes d/dz, $b = d/2$ is the radius of the channel, and the no-slip boundary condition $v_z(b,z) = 0$ has been applied. Note that p' is not automatically a constant as it is for incompressible flow.

Next, the expression for v_z is substituted into the mass equation, (19), which is then formally integrated to obtain an expression for v_r. Eliminating ρ by means of the equation of state leads to

$$v_r(r,z) = \frac{b^2T}{4rp}\frac{\partial}{\partial z}\left[pp'\int_0^r \frac{1}{\mu T}\left(1-\frac{r^2}{b^2}\right)r\,\mathrm{d}r\right]. \tag{25}$$

To proceed further, we note that the solution to (21) satisfying the regularity condition at the origin is $T = T(z)$. This leads to the following simplified expression for v_r:

$$v_r(r,z) = \frac{b^4T}{4rp}\left(\frac{pp'}{\mu T}\right)'\left(\frac{1}{2}\frac{r^2}{b^2}-\frac{1}{4}\frac{r^4}{b^4}\right). \tag{26}$$

The normal velocity boundary condition corresponding to a solid wall is $v_r(b,z) = 0$ implying that

$$\left(\frac{pp'}{\mu T}\right)' = 0 \tag{27}$$

and that $v_r(r,z) = 0$ everywhere. Equation (27) represents one relation between the unknowns $p(z)$ and $T(z)$. A more complicated condition, for instance corresponding to porous flow through the boundary, can be treated in a straightforward manner, but for simplicity we consider only the solid-wall condition.

The final piece of information to complete the solution results from the energy equation, (22). A short calculation yields an equation for $T_1(r,z)$:

$$\frac{1}{r}\frac{\partial}{\partial r}\left(r\kappa\frac{\partial T_1}{\partial r}\right) = -\frac{b^2}{4}\left\{\left[\frac{3}{2}\frac{pp'T'}{\mu T}+p\left(\frac{p'}{\mu}\right)'\right]\left(1-\frac{r^2}{b^2}\right)+\frac{p'^2}{\mu}\frac{r^2}{b^2}\right\}. \tag{28}$$

Equation (28) is solved as follows. To begin, note that for a solution for T_1 to exist, the right-hand side of (28) must satisfy an integrability condition. This condition yields a second relation between p and T and is obtained by forming $\int_0^b r\,\mathrm{d}r$ and using the boundary condition $\kappa\partial T(b,z)/\partial r = \kappa\partial T_1(b,z)/\partial r = q$. (Here, $q > 0$ represents energy input.) The integrability condition is given by

$$q = -\frac{b^3}{16}\left[\frac{3pp'T'}{2\mu T}+p\left(\frac{p'}{\mu}\right)'+\frac{p'^2}{\mu}\right]. \tag{29}$$

3.2. *The case $\mu = const.$*

Equations (27) and (29) can easily be solved for p and T for the case $\mu = \text{const}$. The result is

$$p^2 = p_i^2 - (p_i^2 - p_e^2)\left[(1-Q)\frac{z}{L} + Q\frac{z^2}{L^2}\right], \tag{30}$$

$$T = T_i\left(1 + \frac{2Q}{1-Q}\frac{z}{L}\right), \tag{31}$$

where T_i is the inlet temperature, p_i is the inlet pressure, p_e is the exit pressure and

$$Q \equiv \frac{32\mu L^2 q}{5b^3(p_i^2 - p_e^2)} \tag{32}$$

is a dimensionless heat flux, normalized by the pressure drop along the channel.

The mathematical solution is completed by substituting the expressions for $p^2(z)$ and $T(z)$ into the equation for T_1, (28). This yields

$$\frac{1}{r}\frac{\partial}{\partial r}\left(r\kappa\frac{\partial T_1}{\partial r}\right) = \frac{4q}{b}\left(1 - \frac{r^2}{b^2}\right) + \frac{b^2 p'^2}{4\mu}\left(1 - \frac{2r^2}{b^2}\right) \tag{33}$$

which has as its solution

$$T_1 = \frac{bq}{\kappa}\left[\left(\frac{r^2}{b^2} - \frac{r^4}{4b^4} - \frac{3}{4}\right) + \frac{P}{Q}\left(\frac{r^2}{b^2} - \frac{r^4}{2b^4} - \frac{1}{2}\right)\right] + \tilde{T}(z). \tag{34}$$

Here P is a dimensionless function of z defined as

$$P(z) \equiv \frac{2}{5}\frac{L^2 p'^2(z)}{p_i^2 - p_e^2} \sim O(1). \tag{35}$$

Equation (34) has a homogeneous solution of the form $\tilde{T}(z)$ which cannot be determined until next order in the expansion. However, its value is not required when calculating the heat flux and heat transfer coefficient. Finally in (34), note that $\kappa = \kappa[T(z)]$ to lowest order.

3.3. *Discussion of the case $\mu = const.$*

The LMCF solutions are now complete and can be compared with the corresponding incompressible flow solutions in terms of profiles, flow rates, temperature differences, friction factors and Nusselt numbers.

Consider first the profiles. Summarized below are the LMCF and incompressible flow profiles (including frictional heating) for p, T, and v:

pressure profiles

$$p = \left\{p_i^2 - (p_i^2 - p_e^2)\left[(1-Q)\frac{z}{L} + Q\frac{z^2}{L^2}\right]\right\}^{1/2}, \tag{36a}$$

$$\hat{p} = p_i - (p_i - p_e)\frac{z}{L}; \tag{36b}$$

temperature profiles

$$T = T_i\left(1 + \frac{2Q}{1-Q}\frac{z}{L}\right) + \frac{bq}{\kappa}\left[\frac{r^2}{b^2} - \frac{r^4}{4b^4} - \frac{3}{4} + \frac{P}{Q}\left(\frac{r^2}{b^2} - \frac{r^4}{2b^4} - \frac{1}{2}\right)\right] + \tilde{T}(z); \tag{37a}$$

$$\hat{T} = T_i\left[1+(\hat{Q}+\hat{P})\frac{z}{L}\right]+\frac{bq}{\kappa}\left[\frac{r^2}{b^2}-\frac{r^4}{4b^4}-\frac{3}{4}+\frac{\hat{P}}{\hat{Q}}\left(\frac{r^2}{b^2}-\frac{r^4}{2b^4}-\frac{1}{2}\right)\right]+\tilde{T}(z); \tag{37b}$$

velocity profiles

$$v_z = \frac{b^2(p_i^2-p_e^2)}{8\mu L}\left[\frac{1-Q+2Q(z/L)}{p}\right]\left(1-\frac{r^2}{b^2}\right), \tag{38a}$$

$$\hat{v}_z = \frac{b^2(p_i-p_e)}{4\mu L}\left(1-\frac{r^2}{b^2}\right). \tag{38b}$$

In these expressions, $\hat{}$ denotes the incompressible solution,

$$\hat{Q} \equiv 16\mu L^2 q/b^3 C_p\,\rho T_i(p_i-p_e),\ \hat{P} \equiv (p_i-p_e)/\rho C_p\,T_i,$$

and C_p is the specific heat at constant pressure. As an example the pressure and the velocity are plotted versus z/L in figure 1 for $p_i/p_e = 3$ and various values of Q. There are several points to note. First, p is always greater than $\hat{p}$, implying that p' is smaller as $z\to 0$ and larger as $z\to L$. This follows because heat supplied near the midpoint of the channel ($z\sim L/2$) tends to escape towards each end. The pressure gradient resulting from the heat expansion adds to the applied pressure near the end ($z\sim L$) and subtracts from it near the entrance ($z\sim 0$).

Secondly, observe that when $Q\to 1$, then $p'(0) = 0$ and $v_z(0) = 0$. The implication is that for $Q < 1$ steady-state flow solutions exist with $v_z(z) > 0$ for $0 < z < L$. For $Q > 1$ the flow reverses and there are no physical steady-state solutions (e.g. T becomes negative). Consequently,

$$Q \leqslant 1 \tag{39a}$$

or equivalently

$$q < q_c \equiv \frac{5b^3(p_i^2-p_e^2)}{32\mu L^2} \tag{39b}$$

is required for steady-state LMCF; that is, the heat flux must be sufficiently small that the reverse pressure gradient near the inlet due to heating does not overcome the applied pressure gradient. For the proposed small-scale experiment, we find that $q_c = 16.3\ \mathrm{W\,m^{-2}}$ corresponding to a total heat input along the entire length of the channel of only 5.1 W.

Thirdly, the ordering $Q\sim 1$ implies that $bq/\kappa T_i \sim Pr\,M^2 \ll 1$. Consequently, $T_1/T \ll 1$, thereby justifying the expansion technique used in the solution for T.

Finally, to leading order the LMCF profiles reduce to the incompressible solution for the case $(p_i-p_e)/p_i \ll 1$ and $Q \ll 1$. In addition, by setting $Q = 0$ and treating $(p_i-p_e)/p_i$ as a small parameter we can expand the LMCF pressure and velocity profiles. These profiles reduce exactly to those given in Prud'homme *et al.* (1986) where from the outset the case $Q = 0$, $(p_i-p_e)/p_i \ll 1$ is treated.

The next topic for discussion is the flow rate–pressure drop relation and the corresponding evaluation of the friction factor. The flow rate follows from the usual definition $\dot{m} = 2\pi\int\rho v_z r\,\mathrm{d}r$. As expected, $\dot{m}$ is independent of z for both LMCF and incompressible flow. The values are given by

$$\dot{m} = \frac{\pi b^4(p_i^2-p_e^2)}{16\mu L R T_i} - \frac{2\pi}{5}\frac{Lbq}{RT_i},\quad \hat{\dot{m}} = \frac{\pi\rho b^4(p_i-p_e)}{8\mu L}. \tag{40a, b}$$

The first terms on the right-hand side have different forms but are qualitatively similar in origin; a given pressure drop drives a flow inversely proportional to the viscous

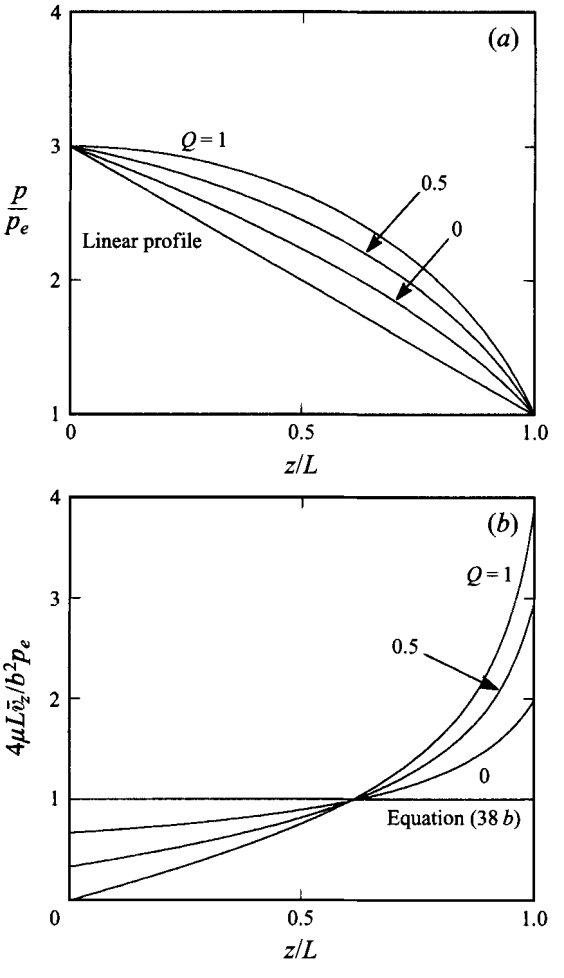

FIGURE 1. (*a*) Helium pressure profile along the channel given by (36*a*). (*b*) Helium velocity profile along the channel given by (38*a*).

friction force. The LMCF, however, has an additional flow-reducing contribution resulting from the reverse pressure gradient due to heat flow. When $q = q_c$, the flow rate reduces to zero.

The friction factor f can be found from the usual definition (Bird *et al.* 1960)

$$f\frac{\overline{\rho v}_z \bar{v}_z}{4b} = -\frac{2\mu}{b}\left(\frac{\partial v_z}{\partial r}\right)_b, \tag{41}$$

where $\bar{U}$ denotes $(2/b^2)\int Ur\,\mathrm{d}r$. In general f can be a function of z. For both LMCF and incompressible flow, however, f is independent of z. Interestingly, in a formal sense, the friction factors are the same for both flows, given by the well-known relation

$$f = \hat{f} = 64/Re, \tag{42}$$

where $Re = \overline{\rho v}_z d/\mu$ and $d = 2b$. In contrast, if one rewrites the friction factor in terms of quantities that can be measured experimentally, the expressions are quite different:

$$f = \frac{10\pi^2 b^5(p_i^2 - p_e^2)}{L\dot{m}(5RT_i\dot{m} + 2\pi Lbq)}, \quad \hat{f} = \frac{4\pi^2 b^5 \rho(p_i - p_e)}{L\dot{m}^2}. \tag{43a, b}$$

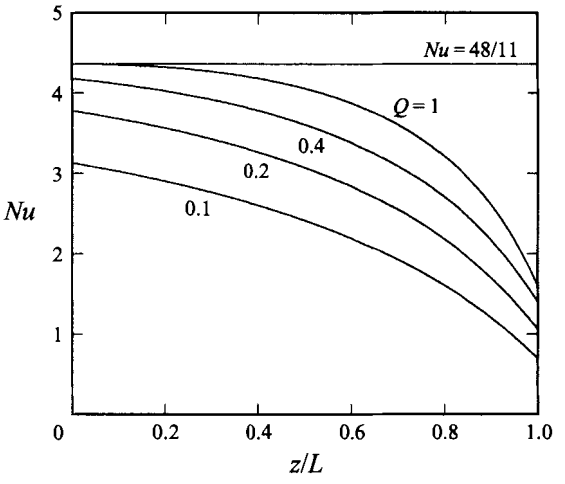

FIGURE 2. Nusselt number along the channel given by (46*a*).

Observe that for LMCF, one is required to measure the inlet temperature and input heat flux, in addition to the pressure drop and flow rate to experimentally determine the friction factor.

The remaining topic of interest concerns the exit temperature and the corresponding Nusselt number. The exit temperatures follow immediately from (37) and are given by

$$T_e \approx T(L) = T_i\left[\frac{5b^3(p_i^2-p_e^2)+32\mu L^2 q}{5b^3(p_i^2-p_e^2)-32\mu L^2 q}\right], \tag{44a}$$

$$\hat{T}_e \approx \hat{T}(L) = T_i\left[1+\frac{p_i-p_e}{\rho C_p T_i}+\frac{16\mu L^2 q}{b^3\rho C_p T_i(p_i-p_e)}\right]. \tag{44b}$$

For a fixed pressure gradient the exit temperature in an incompressible fluid increases linearly with q. For an LMCF fluid, T_e increases even faster with q and approaches infinity as $q \to q_c$. The reason is that as q increases, the flow slows down, allowing the fluid to spend more time getting heated as it moves along the channel.

The Nusselt numbers are easily evaluated from the standard definition (Bird *et al.* 1990)

$$Nu = \frac{d(\partial T/\partial r)_b}{(T)_b-\overline{vT}/\bar{v}} = \frac{2b(\partial T_1/\partial r)_b}{(T_1)_b-\overline{vT}_1/\bar{v}}. \tag{45}$$

In general Nu is a function of z. A short calculation based on (34) yields

$$Nu = \frac{48}{11+6P/Q}, \quad \hat{N}u = \frac{48}{11+6\hat{P}/\hat{Q}}. \tag{46a, b}$$

Although the numerical values for each case are comparable, the LMCF solution is interesting in that $Nu = Nu(z)$ because of the z-dependence of P. For the incompressible case $\hat{P}/\hat{Q} = \text{const.} \ll 1$. This suggests that measurments of Nu or, equivalently the heat transfer coefficient h, from LMCF experiments cannot be made globally from the inlet and exit conditions. Instead, local measurements along the length of the channel are required. Nu is plotted versus z/L in figure 2 for $p_i/p_e = 3$ and various values of Q. Note that the value of Nu along the tube is substantially different from the corresponding incompressible limit $Nu \approx 4.364$.

As a final point, we emphasize that the concept of a steady-state friction factor and heat transfer coefficient only make sense for $q < q_c$. For $q > q_c$ steady state is never achieved and f and h will in general be explicit functions of time until the flow reverses and the system depletes itself of gas.

3.4. *The case $\mu \neq$ const.*

When μ is a function of T, the solutions of the LMCF model exhibit many similar qualitative features to the $\mu =$ const. case. However, the existence of a maximum q defining the boundary of steady-state operation is somewhat more subtle. To show this, we introduce a simple model for μ and κ as follows:

$$\mu = \mu_i \left(\frac{T}{T_i}\right)^{\nu}, \quad \kappa = \kappa_i \left(\frac{T}{T_i}\right)^{\nu}. \tag{47a, b}$$

The transport coefficients are normalized by their inlet values and their variation with T is characterized by the parameter ν. For real gasses $\nu \sim 1$ (for helium used in our proposed test experiment $\nu \sim 0.7$).

The first step in obtaining a solution is to observe from (27) that

$$\frac{pp'}{\mu T} = -c, \tag{48}$$

where c is an integration constant, unknown at this point. The next step is to substitute into (29) to obtain an equation for T. A short calculation gives

$$\frac{\mathrm{d}T}{\mathrm{d}z} = \frac{32}{5}\frac{q}{cb^3}. \tag{49}$$

The solution can be written as

$$T = T_i\left(1 + \lambda \frac{z}{L}\right), \tag{50}$$

where $\lambda = (T_e - T_i)/T_i = 32qL/5cb^3T_i$ is a more physical, but still unknown, constant, replacing c. Observe that T satisfies the inlet condition $T(0) = T_i$ and is linear in z even when $\mu = \mu(T)$.

Equation (50) is substituted back into (48). The resulting relation is easily integrated yielding the following relation for $p(z)$:

$$p^2(z) = p_i^2 - (p_i^2 - p_e^2)\, Q\left\{\frac{[1 + \lambda(z/L)]^{\nu+2} - 1}{(1 + \nu/2)\,\lambda^2}\right\}. \tag{51}$$

Observe that the integration constant has been chosen so that p satisfies the inlet condition $p(0) = p_i$. The unknown constant λ, related to the exit temperature, is determined by requiring $p(L) = p_e$. This gives the desired relation

$$Q = \frac{(1 + \nu/2)\,\lambda^2}{(1 + \lambda)^{\nu+2} - 1}, \tag{52}$$

where, as before $Q = 32\mu_i L^2 q/5b^3(p_i^2 - p_e^2)$. The velocity profile is again given by (24) with $\mu = \mu(T)$.

Equation (52) is plotted in figure 3. Shown here are curves of exit temperature difference *vs.* input heating power (i.e. λ *vs.* Q) for various ν. Note that for $\nu = 0$, corresponding to $\mu =$ const., $T_e - T_i$ is a monotonically increasing function of q as long as $q < q_c$. The condition $q = q_c$ ($Q = 1$) forces $T_e - T_i \to \infty$ and $v_z(0) \to 0$.

However, for $\nu \neq 0$ the exit temperature is a double-valued function of q. Further

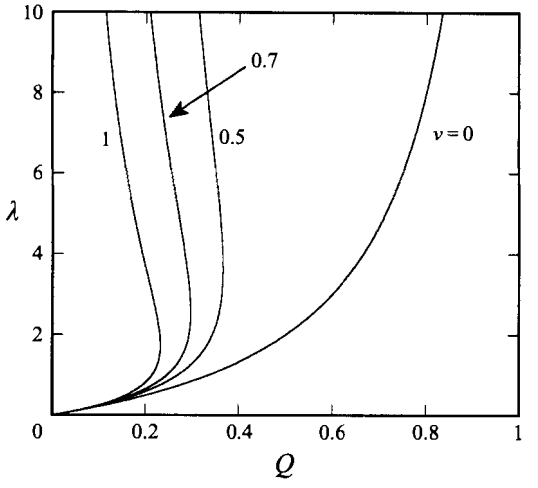

FIGURE 3. Curves of λ versus Q given by (52).

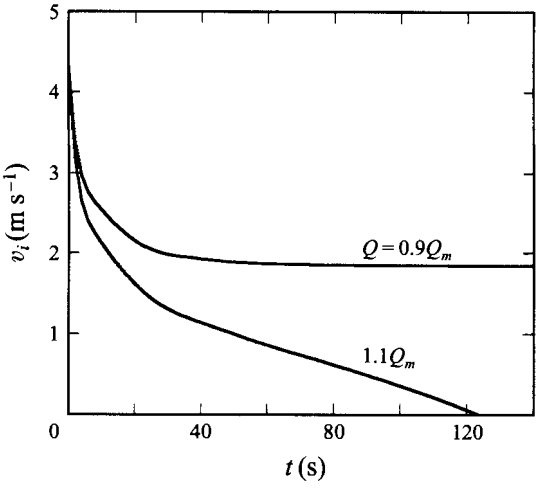

FIGURE 4. Time evolution of the inlet helium velocity for two different values of Q using the parameters of the proposed test experiment.

analysis of the time-dependent one-dimensional model resolves the difficulties as follows. The extremum point where $dQ/d\lambda = 0$ corresponds to a point of marginal stability. The lower branch of the curve is stable for $Q < Q_m$. The upper branch is unstable, perhaps not surprisingly, since in this regime an increase in heating power leads to a reduction in exit temperature.

At the point $Q = Q_m$, $\lambda = \lambda_m$ all the solutions are well behaved – there is no transition to flow reversal nor is the exit temperature approaching infinity. To determine the behaviour for $Q > Q_m$ we have solved the nonlinear time-dependent equations numerically assuming that the source Q is applied at $t = 0$ and using the parameters of the proposed test experiment. The inlet velocity $v_i \equiv \bar{v}_z$ $(z = 0)$ is shown in figure 4 for two cases, one with $Q < Q_m$ and the other for $Q > Q_m$. Observe that when $Q < Q_m$, the inlet velocity evolves to a steady-state value. On the other hand, for $Q > Q_m$, the system never reaches a steady state and just continues to evolve until the flow reverses. Ultimately all the gas is depleted from the system.

It is also worth pointing out that the value of Q_m is substantially reduced as ν increases. For instance, when $\nu = 1$, then $Q_m = \sqrt{3} - \frac{3}{2} = 0.23$ which is much smaller than the value $Q_m = 1$ for $\nu = 0$. Also, for $\nu = 1$ the exit temperature $T_e = (1+\sqrt{3})T_i = 2.73T_i$, representing a finite but not enormous temperature rise.

The mass flow produced by a given pressure drop is obtained by a simple calculation which shows that

$$\dot{m} = \frac{\pi b^4 (p_i^2 - p_e^2)}{8\mu_i LRT_i} \frac{Q}{\lambda} \tag{53}$$

with $\lambda(Q)$ given by (52). This relation is qualitatively similar to the $\mu = \text{const.}$ case, (40*a*). The interesting feature is that the slowest allowable mass flow rate occurs when $Q = Q_m$ and $\lambda = \lambda_m$. This follows because the ratio Q/λ is a decreasing function of Q on the stable portion of the Q *vs.* λ curve. Unlike the $\mu = \text{const.}$ case where $\dot{m} \to 0$ when $Q = Q_m$, in this case $\dot{m}$ achieves a finite minimum value at this point. Thus, for $\nu = 1$, steady-state solutions exist only for

$$\dot{m} > \left(1 - \frac{\sqrt{3}}{2}\right) \frac{\pi b^4 (p_i^2 - p_e^2)}{8\mu_i LRT_i}. \tag{54}$$

The last point of interest is to obtain the friction factor and the Nusselt number. In this case we find the friction factor (given by (42)) is no longer a constant along the channel, since $Re = Re(z)$. The first-order temperature $T_1(r, z)$ and the Nusselt number can again be calculated from (33) and (45) and are given by

$$T_1 = \frac{bq}{\kappa_i}\left(\frac{T_i}{T}\right)^{\nu}\left[\left(\frac{r^2}{b^2} - \frac{r^4}{4b^4} - \frac{3}{4}\right) + \left(\frac{T_i}{T}\right)^{\nu}\frac{P}{Q}\left(\frac{r^2}{b^2} - \frac{r^4}{2b^4} - \frac{1}{2}\right)\right] + \tilde{T}(z), \tag{55}$$

$$Nu = \frac{48}{11 + 6(T_i/T)^{\nu} P/Q}, \tag{56}$$

where P is given by (35).

3.5. *A simple model for turbulent flow*

Some of the effects of turbulent flow can be incorporated into the one-dimensional model by the simple procedure of introducing a turbulent friction factor. Consistent with the LMCF expansion we easily obtain a set of one-dimensional equations for $\rho(z), T(z), p(z), \bar{v}_z(z)$:

$$\rho\bar{v}_z = \frac{\dot{m}}{\pi b^2} = \text{const.}, \tag{57}$$

$$\frac{\mathrm{d}p}{\mathrm{d}z} = -\frac{f\rho\bar{v}_z^2}{2d}, \tag{58}$$

$$\tfrac{3}{2}R\rho\bar{v}_z\frac{\mathrm{d}T}{\mathrm{d}z} + p\frac{\mathrm{d}\bar{v}_z}{\mathrm{d}z} = \frac{2q}{b} - \bar{v}_z\frac{\mathrm{d}p}{\mathrm{d}z}, \tag{59}$$

$$p = R\rho T. \tag{60}$$

Here,

$$\bar{v}_z \equiv \frac{2}{b^2}\int_0^b v_z r\,\mathrm{d}r. \tag{61}$$

There is as yet no detailed experimental determination of f in the LMCF regime with non-zero heat input or for that matter even a determination that the dominant effect of turbulence can be modelled by merely modifying the friction factor. Even so, to

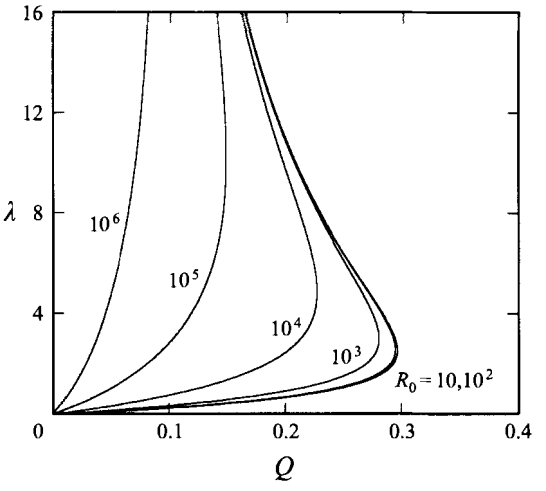

FIGURE 5. Curves of λ versus Q given by (64).

obtain some preliminary insight we shall, as is common practice in porous-medium flow, use such a friction factor and for want of anything better set $f = 64/Re + f_\infty$. Here, $f_\infty = \text{const.} \approx 0.07$ is the friction factor in the turbulent regime, corresponding to a rough tube.

The solution is obtained as follows. Using the fact that $\rho \bar{v}_z = \text{const.}$ allows us to immediately integrate (59), yielding an expression for $T(z)$ given by

$$T(z) = T_i\left(1+\lambda\frac{z}{L}\right), \tag{62a}$$

$$\lambda = \frac{T_e - T_i}{T_i} = \left(\frac{4\pi bL}{5RT_i}\right)\frac{q}{\dot{m}}. \tag{62b}$$

The temperature profile is again linear in z, irrespective of the value of f, although $\lambda = \lambda(f)$.

The expression for T is substituted into the momentum equation which can also be easily integrated leading to an expression for p that can be written as

$$p^2(z) = p_i^2 - \frac{RT_i L}{2b}\left(\frac{\dot{m}}{\pi b^2}\right)^2 \int_0^{z/L} f(1+\lambda\xi)\,\mathrm{d}\xi. \tag{63}$$

As before the relation between λ and Q (i.e. exit temperature and heat flux) is obtained by setting $p(L) = p_e$. In normalized form, this relationship is given by

$$\frac{f_\infty R_0}{32}(1+\lambda/2)\,Q^2 + \frac{[(1+\lambda)^{2+\nu}-1]}{(1+\nu/2)}Q - \lambda^2 = 0, \tag{64}$$

where Q has been defined in conjunction with (52) and R_0 is a dimensionless parameter related to Reynolds number, defined by

$$R_0 = \frac{b^3(p_i^2 - p_e^2)}{4\mu_i^2 RT_i L}. \tag{65}$$

For the proposed test experiment $R_0 \approx 1300$.

The goal now is to examine (64) to determine how the modification of the friction factor alters the laminar theory conclusions regarding the existence of a maximum q for steady-state solutions. This basic question is answered in figure 5 where we have

plotted curves of λ *vs.* Q for various R_0. Observe that the qualitative nature of the curves remains unchanged as the turbulence (i.e. R_0) increases. As $R_0 \to 0$ the laminar result is recovered. For large R_0 the maximum normalized heat flux decreases with R_0 while the exit temperature increases.

The basic conclusion is that in the simple turbulent model discussed here important quantitative changes in LMCF properties occur, but the qualitative behaviour remains the same. Specifically, for steady-state flow the applied heat flux must lie below a critical value, indicating that the effect is not an obvious pathology of the laminar flow assumptions.

4. Conclusions

We have investigated the basic properties of a relatively uncommon regime of fluid dynamics, low Mach number compressible flow. This regime, which is of importance in the cooling of large-scale superconducting magnets, is characterized by an enormous aspect ratio $L/d \sim 10^6$. The consequence is that friction dominates inertia, leading to highly subsonic flows, even though finite pressure, temperature, and density gradients are required because of the exceptionally long lengths involved. Many features of the flow are qualitatively similar, although quantitatively different from incompressible flows. Perhaps the most surprising result is that steady-state solutions exist only below a critical value of heat input. Above this value the compressibility leads to a flow reversal against the applied pressure gradient causing the gas to flow out of both the inlet and outlet, thereby depleting the coolant. The existence of a maximum heat input and a corresponding minimum flow rate are found under both laminar and simple turbulent conditions. Parameters have been given for a simple small-scale experiment, that could test several of the conclusions of the theory and we intend to do so in the future.

The authors would like to thank Professor P. Rosenau for several very useful discussions. This work was partially supported by the Office of Fusion Energy in the Department of Energy.

REFERENCES

BERG, H. R. VAN DEN, SELDAM, C. A. TEN & GULIK, P. S. VAN DER 1993 *J. Fluid Mech.* **246**, 1–20.

BIRD, R. B., STEWART, W. E. & LIGHTFOOT, E. N. 1960 *Transport Phenomena.* John Wiley & Sons.

FOUMENY, E. A. & MA, J. 1994 *Chem. Engng Technol.* **17**, 50–60.

KAVIANY, M. 1991 *Principles of Heat Transfer in Porous Media.* Springer.

PRINS, H. J. 1991 The optimal model for a non-Newtonian compressible gas. *Rep. Fac. of Techn. Math. & Informatics.* Delft Univ. of Technol.

PRUD'HOMME, R. K., CHAPMAN, T. W. & BOWEN, J. R. 1986 *Appl. Sci. Res.* **43**, 67.

SHAJII, A. & FREIDBERG, J. P. 1994*a* *J. Appl. Phys.* **76**, 3149.

SHAJII, A. & FREIDBERG, J. P. 1994*b* *J. Appl. Phys.* **76**, 3159.

THOME, R. J. 1994 *IEEE Trans. Mag.* **30**, 1595–1601.

WHITE, F. M. 1986 *Fluid Mechanics.* McGraw-Hill.

WHITE, F. M. 1991 *Viscous Fluid Flow*, pp. 173–190. McGraw-Hill.

ZANOTTI, F. & CARBONELL, R. G. 1984 *Chem. Engng Sci.* **39**, 299–311.